J. Fluid Mech. (1982), *vol.* 114, *pp.* 157–173
Printed in Great Britain

Formation of thermoclines in zero-mean-shear turbulence subjected to a stabilizing buoyancy flux

By E. J. HOPFINGER† AND P. F. LINDEN
Department of Applied Mathematics and Theoretical Physics, University of Cambridge

(Received 13 February 1981)

Laboratory experiments in which a stabilizing buoyancy flux is imposed on zero-mean-shear turbulence generated by an oscillating grid are discussed. The buoyancy flux is imposed at the top of a water column either as a constant heat flux or by the continuous addition of fresh water at the top of a salt solution. Two types of experiments were carried out. In the first, the oscillating grid was positioned near the buoyancy input plane at the top of the water column to represent an input of turbulence kinetic energy near the surface. In this case a mixed layer was formed which extended from the surface down to a finite depth, and was bounded below by a stable thermocline. The mixed-layer depth remained constant in time but, contrary to earlier suggestions, was not found to be proportional to the Monin–Obukhov length. Instead the depth of the mixed layer was found to depend on the rate of decay of the turbulent kinetic energy with depth through the mixed layer. A second set of experiments was carried out with the grid positioned well below the surface to represent turbulence produced by bottom stirring. At low values of the buoyancy flux the fluid column remained well mixed, but once the buoyancy flux exceeded a critical value a stable stratification built up near the surface. Under certain conditions, a steady stratification was produced in which the diffusive flux balanced the turbulent flux in the mixed layer below. At larger values of the buoyancy flux, the diffusive flux is not large enough to remove the buoyancy from the surface and a 'runaway' stratification develops. The criterion for the formation of surface stratification is also found to depend on the rate of decay of the turbulent kinetic energy with depth, and the implications of this work for the formation of fronts produced by tidal stirring are discussed.

1. Introduction

The formation of the seasonal thermocline during the summer and the production of coastal fronts by tidal stirring, are two oceanic examples of the combined effects of turbulence and a stabilizing buoyancy flux. Heat is absorbed near the surface of the sea and mixed downwards by the turbulence generated by the wind, producing an upper mixed layer bounded below by a relatively sharp density (temperature) change. In shallow water this thermocline is also effected by turbulence generated at the bottom by tidal currents. If the turbulence is sufficiently energetic it can mix the whole water column, thereby producing a front between the mixed and stratified water. If advective effects are unimportant these processes can be considered in terms of the interaction between the locally generated turbulence and the local buoyancy flux.

† On leave from Institute de Mécanique, Université Scientifique et Medicale de Grenoble.

In recent years there have been many studies of the oceanic thermocline (and equivalently the rise of the atmospheric inversion). Most of this work has been restricted to one-dimensional (or local) models, ignoring variations in the horizontal (see Kraus 1977), and has considered the effects of turbulence on a fluid layer where the initial stratification is specified. However, in many naturally occurring situations the stratification evolves as the turbulence transports a stable buoyancy flux, and it is this aspect of the problem that is addressed in this paper.

Consider the case when the surface is being heated at a constant rate, and the rate of input of mechanical energy by the wind is constant. Heating tends to reduce the depth of the thermocline and the mixing produced by the turbulence tends to deepen it. Thus it is plausible that a depth exists at which these two opposing effects balance and a steady-state is achieved. Some experiments of the type discussed in this paper supporting the idea of a steady mixed layer depth have recently been reported by Kantha & Long (1980). Kitaigorodskii (1960) suggested, from dimensional considerations, that this depth is given by

$$D = au_*^3/B, \tag{1.1}$$

where u_* is the friction velocity, B is the stabilizing buoyancy flux and a is a constant. Using selected oceanic data Kitaigorodskii found $a \simeq 2$. As pointed out by Kraus & Turner (1967), (1.1) implies that a constant fraction of the kinetic energy input is being used to change the density of the mixed layer, and D is proportional to the Monin–Obukhov length.

Although this is a very appealing idea, to our knowledge there has not been a convincing test of this scaling. Turner & Kraus (1967) carried out experiments using a variable buoyancy flux B and found qualitative agreement with (1.1) i.e. when the buoyancy flux increased the depth of the mixed layer decreased, and vice versa. However, there are good reasons to suspect that the mixed-layer depth will not be determined by (1.1), at least under some circumstances. For example, in the case of tidal mixing, the buoyancy flux is put in at the surface, whilst the turbulence is generated at the bottom. Consequently, the rate at which turbulent energy is made available for mixing at the surface will, in general, depend on the water depth and may not be a constant fraction of u_*^3. Furthermore, it is known that turbulence is a very inefficient mixer: most of the energy is dissipated viscously. It is only a small fraction of the mechanical energy input which is used to work against the buoyancy forces, and there is no *a priori* reason to expect that this fraction is a constant. The experiments by Kantha & Long (1980) show that the relationship between the mixed-layer depth and the surface parameters depends upon the rate of decay of turbulent kinetic energy with depth. Their results are not consistent with a Monin–Obukhov scaling of the form given in (1.1), although these authors concluded otherwise.

In this paper we describe the results of some laboratory experiments on the combined effects of turbulence and a stabilizing buoyancy flux. As in Kantha & Long's experiments the turbulence is generated by the vertical oscillation of a horizontal grid of bars. This produces a horizontally homogeneous field of turbulence, whose r.m.s. turbulent velocity u decreases linearly with distance from the grid. In an unstratified fluid the scale of the turbulence l increases linearly with distance from the grid so that the eddy viscosity $K = ul$ is constant in space. The buoyancy flux is produced either by adding fresh water at the top of a salt solution, or by heating the

water over a horizontal plane. By changing the position of the grid relative to the position of the buoyancy flux input it was possible to examine the effects of both surface- and bottom-generated turbulence.

The laboratory experiments are described in § 2 and the results presented in § 3. A local energy balance, in which the viscous decay of the turbulence away from the oscillating grid is taken explicitly into account, is discussed in § 4. The conclusions and implications of the experiments are given in § 5.

2. The experiments

2.1. *The apparatus*

The experiments were carried out in the mixing tank used by McDougall (1979), which is a copy of the tank described by Turner (1968). The tank is 25·4 cm by 25·4 cm in cross-section and 45 cm deep. Turbulence is generated by oscillating a horizontal grid of square bars (1 cm in cross-section with a 5 cm mesh length) vertically about its mean position. The frequency of the grid oscillation was adjusted between 1 Hz to 6 Hz, and the stroke was set at 1 cm, 2·4 cm and 4 cm, in order to cover a range of turbulence velocity and length scales.

A stabilizing buoyancy flux was produced in two ways. One method was to add fresh water continuously to the top of a column of salt solution. The fresh water was introduced through a 1 cm thick sheet of foam rubber placed on the surface of the salt water, which served to keep the flux of fresh water uniform over the cross-section. Mixed fluid was withdrawn through four holes in the side of the tank, thus keeping the depth of the water column constant during an experiment (see figure 1 *a*). The buoyancy flux $B_0' = g\Delta\rho_0 V/\rho$, where V is the velocity (volume flux/unit area) at which lighter fluid is supplied at the surface, $\Delta\rho_0/\rho$ the fractional density difference between the fresh and salt water and g the gravitational acceleration.

Alternatively, a stabilizing buoyancy flux was produced by heating the top of the water column. Heat was introduced by means of a 110 ohms heating grid located at a depth d below the water surface, as shown on figures 1 (*b*, *c*). The heating grid consisted of a 0·4 mm diameter enamelled wire and had a 1·4 cm mesh. The grid was connected to a variable a.c. power supply. The water surface and the side walls of the tank were insulated with sheets of expanded polystyrene. In this case the buoyancy flux $B_0' = g\alpha q_0/\rho c_p$, where q_0 is the heat flux/unit area, α the coefficient of thermal expansion and c_p the specific heat.

Experiments were conducted with the oscillating grid near the buoyancy input plane (figures 1 *a*, *b*) which represents surface stirring, or with the grid some distance from the buoyancy input (figure 1 *c*) which produces conditions which model bottom-generated turbulence. In each case the oscillating grid was started and when the turbulence was fully established (after a few minutes), the mass flux or heat flux was suddenly switched on. With a few exceptions the buoyancy flux was maintained at a constant value throughout an experiment.

The mixed-layer depth was measured from a shadowgraph, and by the addition of dye. Salinity profiles were measured by withdrawing 1 ml samples at predetermined depths, and analysing them with a refractometer. Thermistors were used to measure the temperature at fixed points in the water column and vertical profiles were obtained by traversing.

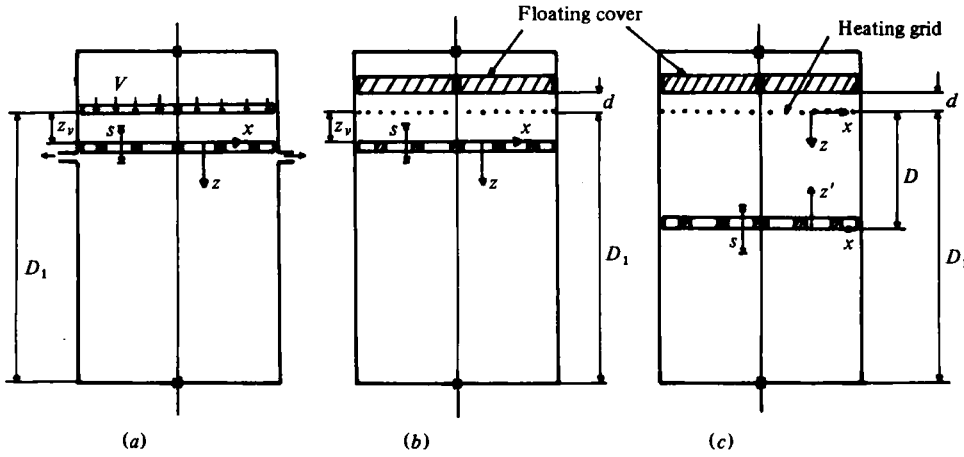

FIGURE 1. A sketch of the stirring tank and the experimental arrangement for the three types of experiment. (*a*) Surface stirring and buoyancy flux due to the addition of fresh water at the top of a salt layer. (*b*) Surface stirring and a stabilizing heat flux. (*c*) Bottom stirring and a stabilizing heat flux.

2.2. *Turbulence characteristics in the absence of buoyancy effects*

Before discussing the interaction between the turbulence and the stabilizing buoyancy flux, it is necessary to describe the turbulent field in an unstratified fluid. Measurements of the turbulent velocity field produced by the oscillating grid were made by Thompson & Turner (1975) and by McDougall (1979), whilst Hopfinger & Toly (1976) have measured the turbulence produced by this grid and also a scaled-up grid in a much larger tank. Hopfinger & Toly showed that the r.m.s. horizontal velocity u(cm s^{-1}) at distance z(cm) from a virtual origin could be described by the empirical formula

$$u = CfS^{\frac{3}{2}}M^{\frac{1}{2}}z^{-1}. \tag{2.1}$$

Here f(Hz) is the frequency of grid oscillation, S(cm) the stroke, and M(cm) the mesh length. The virtual origin $z = 0$ was found to be 0·5–1·0 cm behind the mid-plane of the grid. The coefficient of proportionality C was measured to be 0·20 by Thompson & Turner using a stroke $S = 1$ cm, and we use this value for our experiments with $S = 1$ cm and 2·4 cm. At the largest value of the stroke ($S = 4$ cm), we take $C = 0{\cdot}30$ which is the value obtained by Hopfinger & Toly at larger strokes. The r.m.s. vertical velocity w was measured to be proportional to u, with $w/u \simeq 1{\cdot}25$ for $z \gtrsim M$.

The integral scale of the turbulence l was found to increase linearly with distance from the virtual origin i.e. $l = \beta z$. The coefficient β is a function of the stroke S, for a given grid geometry, and was measured to be $\beta = 0{\cdot}1$ when $S = 1$ cm and $\beta = 0{\cdot}25$ when $S = 4$ cm. On the basis of linear interpolation we take $\beta = 0{\cdot}17$ when $S = 2{\cdot}4$ cm. Using dimensional analysis, Long (1978) introduced the grid action parameter $K_1 = uz$, where K_1 is a constant for large Reynolds number. From (2.1), $K_1 = CfS^{\frac{3}{2}}M^{\frac{1}{2}}$ which appears naturally as $u_0 z_0$ (see (2.4)).

The observed spatial decay of the turbulence intensities (2.1) allows us to estimate the magnitude of the terms of the turbulent kinetic energy equation. As these estimates will be useful when examining the effects of stratification we shall discuss them here.

The turbulent kinetic energy equation of an unstratified flow without mean shear is

$$\frac{d}{dz}\left(\frac{1}{\rho}\overline{w'p'}+\tfrac{1}{2}\overline{w'q^2}\right)+\epsilon=0, \tag{2.2}$$

where w' is the instantaneous vertical velocity, p' the pressure fluctuation, $\frac{1}{2}q^2$ the turbulent kinetic energy/unit mass, ϵ the rate of dissipation and ρ the fluid density. Writing $(\rho^{-1}\overline{w'p'}+\frac{1}{2}\overline{w'q^2})=ru^3$ and $\epsilon=Au^3/l$, where A is a constant of order unity, (2.2) becomes

$$\frac{du^3}{dz}=-\frac{b}{\beta}\frac{u^3}{z}, \tag{2.3}$$

where $b=A/r$. The solution is

$$u=u_0(z/z_0)^{-b/3\beta}. \tag{2.4}$$

Thus when $u\propto z^{-1}$ as in (2.1), $b/\beta=3$.†

We use this last result to obtain an estimate of the relative importance of the pressure and diffusive transports in (2.2), which, in general, depend upon the flow under consideration. If we make the reasonable assumption that $\overline{w'q^2}=\frac{1}{2}wq^2$, write $\rho^{-1}\overline{w'p'}=\frac{1}{2}k\overline{w'q^2}$ and use the observed relation $w=1{\cdot}25u$, then we find that the coefficient r takes the value $r=1{\cdot}1\times(1+k)$. This implies that $A=3{\cdot}3(1+k)\beta$, and since $\beta\simeq 0{\cdot}2$ we find that A is approximately 1 provided $k\sim 1$. From this indirect argument we deduce that the two transport terms are of equal order. In our subsequent analysis (§ 4) a value of $r=2{\cdot}2$ will be used, which corresponds to $k=1$.

3. Observed mixed-layer depth and density structure

3.1. *Surface stirring*

When the turbulence is generated close to the top of the water column where the stabilizing buoyancy flux is imposed, the buoyancy is transported downwards a finite distance by the turbulent motions and a surface mixed layer of depth D' is produced (see figure 1*a*, *b*). The mixed layer was visible on the shadowgraph shortly after the buoyancy flux was established, and remained constant in depth as long as the buoyancy flux was held constant. Beneath the mixed layer the turbulent motions rapidly died out and, in time, an interfacial layer or thermocline developed at the base. The frontal zone between the mixed layer and the lower non-turbulent fluid was variable in structure, and internal waves trapped in the interfacial layer were visible.

The formation of the mixed layer and the development of the thermocline is revealed by temperature profiles as shown on figure 2. The profiles show that the temperature of the mixed layer increases with time, but the mixed-layer depth remains constant provided the buoyancy flux and stirring are held at a fixed value. In this example the experiment lasted some 30 minutes, and constant mixed-layer depths were observed over longer periods in other runs.

The thickness of the thermocline also appears, from figure 2, to remain constant in time. Figure 3 shows a number of vertical density profiles from different experiments which have been non-dimensionalized by the density difference across the thermocline

† This experimental result implies that, since $\beta=\beta(s)$, the assumption of a constant value of r is not, strictly speaking, correct. In addition at low Reynolds numbers, A decreases slightly with decreasing Reynolds number. In practice, both r and A vary slowly with stroke and may be taken as constant.

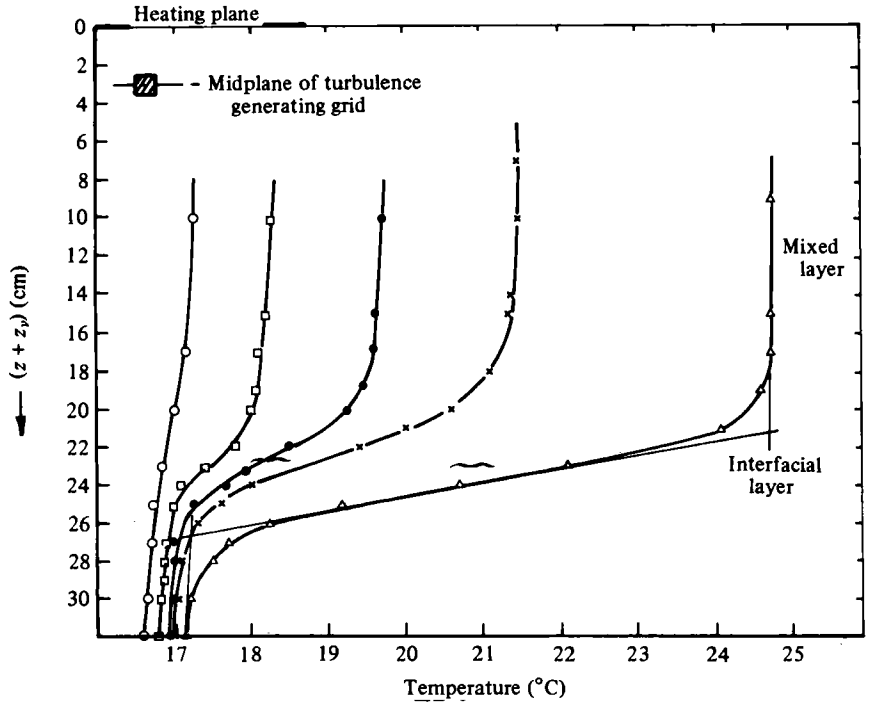

FIGURE 2. A set of temperature-depth profiles measured during a single experiment with surface stirring. Note that the depth of the mixed layer remains constant throughout the experiment. $(Sf)^3/B_0' = 89400$ ○, 1 min after initiation of heat flux; □, 3 min; ●, 6 min; ×, 10 min; △, 27 min. ~ mixed-layer depth determined from shadowgraph.

and the mixed-layer depth D. Plotted in this way the profiles take a universal form, and the thermocline thickness is seen to be approximately 0·3 D. This result is the same for both temperature and salinity interfaces.

Although the mixed layer usually lives up to its name, so that density variations, if any, are within the resolution of the measurements, under stable conditions when the buoyancy flux is high a measurable density gradient is observed in the mixed layer. An example showing this density gradient is the profile denoted by triangles on figure 3. The magnitude of the temperature gradient in the mixed layer (when measurable) is plotted on figure 4 against $q/\rho c_p uz$, the heat flux per unit area q at the depth of the virtual origin divided by $\rho c_p uz$, where c_p is the specific heat, which is a measure of the eddy viscosity based on a length scale of order z. From this figure we see that $q \simeq \rho c_p uz\, dT/dz$, which suggests that the heat flux is transported by eddies of size z. Since the integral scale of the turbulence $l \ll z$, the energy of these large-scale eddies is small, but it appears that they are efficient at transporting heat through the mixed layer.

The global energy argument leading to (1.1) implies that the mixed-layer depth D' should be proportional to $(Sf)^3/B_0'$. In figure 5 it is shown that, although D' does increase with $(Sf)^3/B_0'$, the dependence is much weaker than is implied by the global energetics. Furthermore, the scatter in the data far exceeds the experimental error. We shall show in § 4 that a more appropriate scaling can be found when the decay of the turbulence with distance from the surface is included.

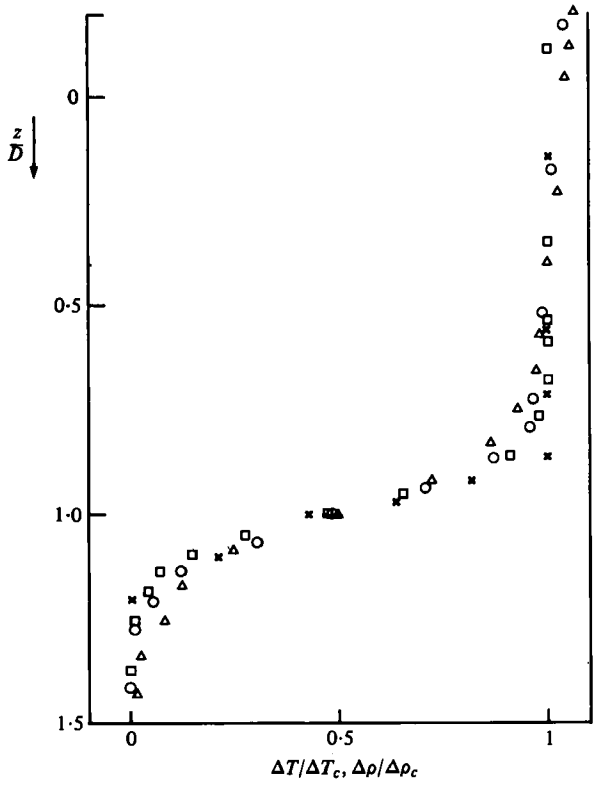

FIGURE 3. Dimensionless temperature profiles produced by surface stirring from four different experiments. The depth has been scaled by the mixed-layer depth D, and the temperature by the temperature difference ΔT_c between the mixed layer and the ambient fluid below. The Peclet number for each experiment was: △, 165; ×, 104; ○, 918; □, 931. l at $z/D = 1$ varied from 1 to 3·6 cm.

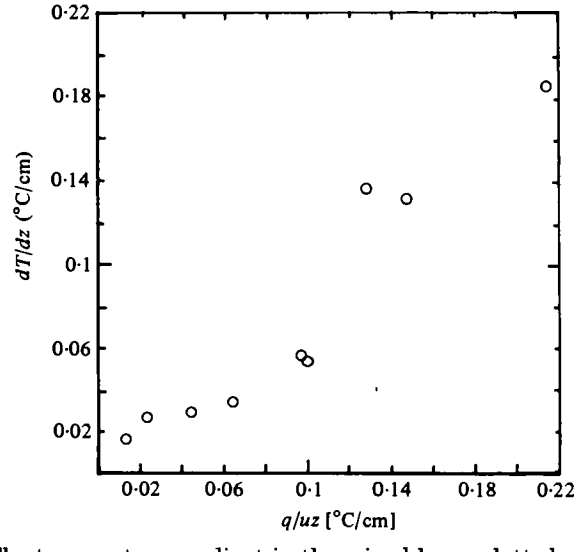

FIGURE 4. The temperature gradient in the mixed layer plotted against $q/uz\rho c_p$ where q is the heat flux across the plane of the virtual origin ($z = 0$).

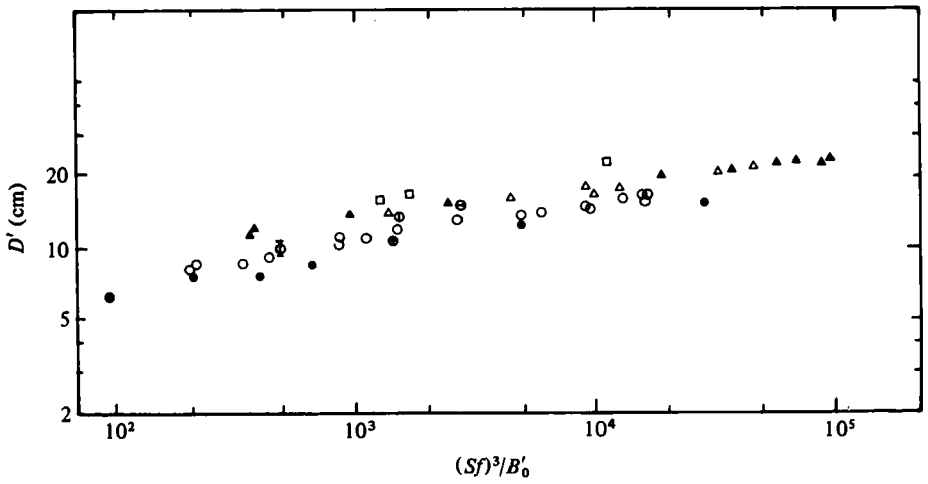

FIGURE 5. The mixed layer depth D' plotted against $(Sf)^3/B_0'$, where S is the stroke, f the frequency and B_0' the buoyancy flux. Different symbols correspond to different values of S and the virtual origin location z_v with respect to the buoyancy input plane.

	Mass flux					Heat flux		
	○	⊙	⊖	⊕	△	●	▲	□
S(cm)	1	1	1	1	2·4	2·4	2·4	4
z_v(cm)	1·5	2·5	3·5	0·8	2·5	1·4	2·5	2·5

3.2. *Bottom stirring*

In this case the turbulence is generated at a depth D below the heating plane as shown in figure 1(*c*). When the imposed buoyancy flux is weak, the heat is mixed downwards by the turbulent motion and the whole water column is maintained at a uniform temperature. This case is shown in figure 6(*a*) which is a plot of the 'surface' temperature T_s (measured by a thermistor located 0·5 cm below the free surface) against time for $(Sf)^3/B_0' = 1{\cdot}5 \times 10^5$. The broken line corresponds to the rate of increase of temperature which would be measured if the total water column remained vertically mixed. At larger values of the buoyancy flux, the surface temperature increases at a much higher rate than that predicted for a well-mixed water column as shown on figures 6(*b*, *c*) for $(Sf)^3/B_0' = 1{\cdot}6 \times 10^4$ and $3{\cdot}2 \times 10^3$, respectively. In these cases the turbulence is no longer sufficiently energetic to mix the heat downwards and a stable surface density stratification develops. The temperature fluctuations increase with increasing heat flux (compare figures 6*a*, *b*) until the stratification becomes so strong that the turbulent eddies can no longer penetrate to the surface. In this case (figure 6*c*), the surface temperature increases relatively smoothly and leads to a 'runway' situation with the surface temperature and the stratification increasing indefinitely.

At values of $(Sf)^3/B_0'$ lying between the conditions for the onset of stratification and the 'runaway' situation an equilibrium temperature gradient develops. This situation is shown on figure 7 where the surface temperature is plotted as a function of time for an experiment with $(Sf)^3/B_0' = 4{\cdot}1 \times 10^4$. After the initial rate of increase of T_s which far exceeds the rise in the temperature of the equivalent mixed column T_B (shown by the broken line), the rate of increase of T_s becomes approximately equal to the rate of increase of T_B as can be seen by comparing the slopes of the two curves for

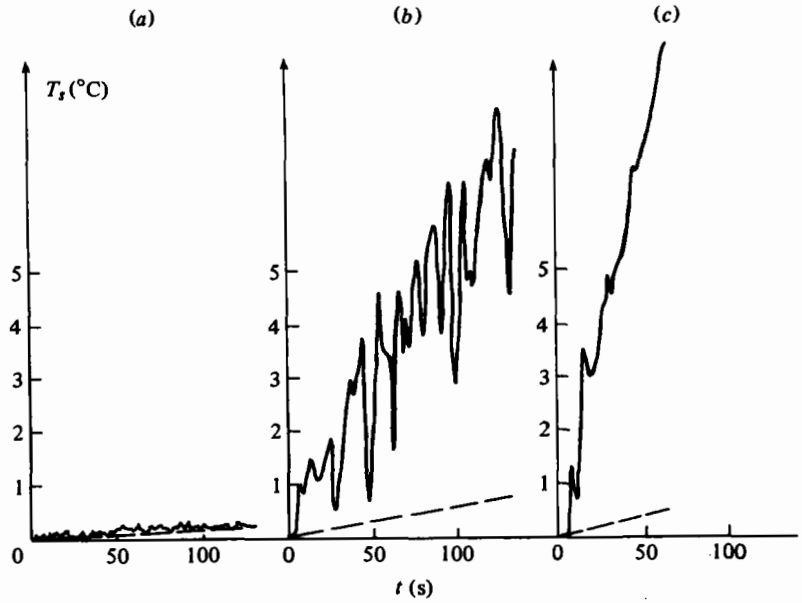

FIGURE 6. The increase in surface temperature with time produced by bottom stirring for three values of $(Sf)^3/B_0'$: (*a*) $1{\cdot}5\times10^5$; (*b*) $1{\cdot}6\times10^4$; (*c*) $3{\cdot}2\times10^3$. The broken line corresponds to the temperature that would have been measured if the heat were redistributed throughout the whole fluid column.

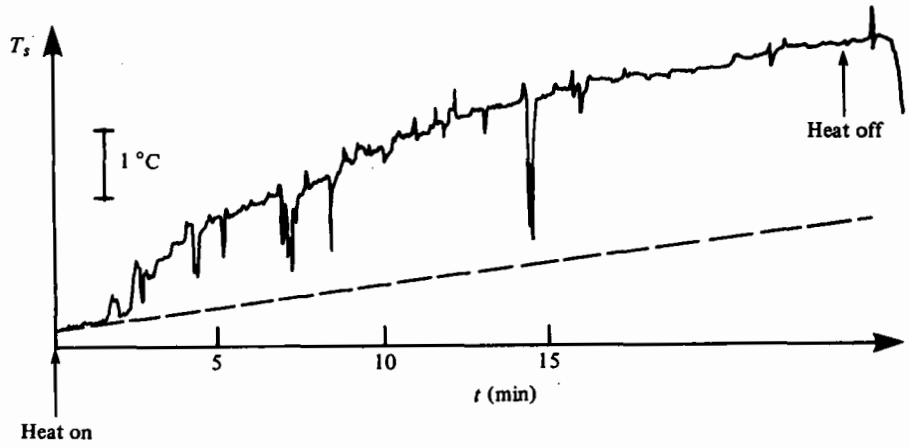

FIGURE 7. Rate of increase in surface temperature as a function of time for $(Sf)^3/B_0' = 4{\cdot}1\times10^4$, corresponding to $CD^4B_0/(u_0z_0)^3 = 7{\cdot}05$. The surface temperature increases at a decreasing rate as time increases and after about 16 min increases at the same rate as the bulk temperature.

$t \geqslant 15$ minutes. Thus, although the water column is still stratified, the temperature gradient adjusts so that the heat put in at the surface can again be redistributed throughout the water column. This example shows that the rate of change of the surface temperature depends on the history of the system as was first demonstrated by Kraus & Turner (1967). We shall return to this point in the discussion when we examine some of the consequences of this work for the ocean.

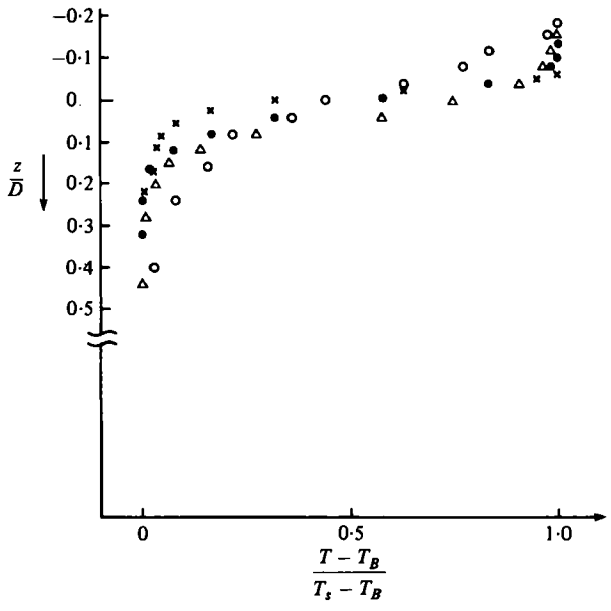

FIGURE 8. Dimensionless temperature-depth profiles produced by bottom stirring. ○, $(T_S - T_B)$ = 1·8 °C, D = 12·5 cm; △, 13·25 °C, D = 12·5 cm; ●, 2·65 °C, D = 12·5 cm; ×, 10·9 °C, D = 18 cm.

In figure 8 vertical temperature profiles are plotted in non-dimensional form. The temperature excess at the surface has been set equal to unity, and the depth non-dimensionalized by D which is the distance of the grid from the heating plane. Between the heating plane and the free surface, the temperature is uniform due to the convective motion produced above the heating grid. Beneath this uniform region a stable thermocline develops which, as in the case of surface stirring, scales on depth D. The region beneath the thermocline remains well mixed.

4. Local-flux balance model

4.1. *Mixed-layer depth*

In the previous section it was noted that the observed mixed-layer depths were at variance with the predictions of global energetics. In their traditional form global models related the mixed-layer depth to the buoyancy flux and the friction velocity *at the surface*, whilst the interaction of the turbulence with the buoyancy flux is strongest near the thermocline. Linden (1975) showed that it was necessary to allow for the decay of the turbulence with distance from the surface when estimating the rate of advance of a mixed layer into a stratified fluid. This approach recognizes the essentially local nature of the interaction of the turbulence with the stratification near the thermocline and is the one adopted here.

In the presence of a buoyancy flux, the turbulent energy equation (2.2) becomes

$$\frac{d}{dz}\left(\frac{1}{\rho}\overline{w'p'} + \tfrac{1}{2}\overline{w'q^2}\right) = g\overline{w'\rho'}/\rho - \epsilon, \tag{4.1}$$

where ρ and ρ' are the mean and fluctuating densities, respectively. Making the same assumptions as in § 2.2, (4.1) takes the form

$$r\frac{du^3}{dz} = -\frac{A}{\beta}\frac{u^3}{z} + \frac{g}{\rho}\overline{w'\rho'}. \tag{4.2}$$

In the mixed layer the density is (by definition) independent of height, and so the buoyancy flux is a linear function of height, i.e.

$$\frac{g}{\rho}\overline{w'\rho'} = \frac{B_0}{D}(z-D). \tag{4.3}$$

Here the buoyancy flux B_0 is referred to the virtual origin and is related to the input flux B_0' by

$$B_0 = B_0' D/(D+z_v), \quad \text{mass flux;}$$
$$B_0 = B_0' DD_1/(D_1+d)(D+z_v), \quad \text{heat flux}$$

(see figure 1*a*, *b*).

Substituting (4.3) into (4.2) and solving the resulting equation for u, we get

$$\left(\frac{u}{u_0}\right)^3 = \left(\frac{z}{z_0}\right)^{-b/\beta}\left\{1-\frac{1}{r}\left(\frac{z}{z_0}\right)^{b/\beta}\frac{B_0}{Du_0^3}\left[\frac{Dz}{(1+b/\beta)}\left(1-\left(\frac{z_0}{z}\right)^{1+b/\beta}\right)-\frac{z^2}{(2+b/\beta)}\left(1-\left(\frac{z_0}{z}\right)^{2+b/\beta}\right)\right]\right\}. \tag{4.4}$$

Here we have written $b = A/r$ (as in § 2) and applied the boundary condition that $u = u_0$ at $z = z_0$.

We assume that, in the mixed layer $z < D$ where the vertical density gradient is weak, the ratio b/β takes the same value as in the neutral case, i.e. $b/\beta = 3$. Then, when $(z/z_0)^4 \gg 1$, (4.4) reduces to

$$\left(\frac{u}{u_0}\right)^3 = \left(\frac{z_0}{z}\right)^{-3}\left[1-\frac{1}{r}\frac{B_0 z^4}{D(u_0 z_0)^3}\left(\frac{D}{4}-\frac{z}{5}\right)\right]. \tag{4.5}$$

Mixing stops at the base of the mixed layer, and (4.5) shows that $u = 0$ when $z = D$ when

$$D = (20r)^{\frac{1}{4}}(u_0 z_0)^{\frac{3}{4}} B_0^{-\frac{1}{4}}. \tag{4.6}$$

Equation (4.5) shows that the mixed-layer depth scales on $(u_0^3/B_0)^{\frac{1}{4}}$, for fixed z_0, rather than u_0^3/B_0 as suggested by Monin–Obukhov scaling. The $\frac{1}{4}$ power is a consequence of the neutral decay law $u \propto z^{-1}$. For example, a decay law of the form $u \propto z^{-\frac{3}{4}}$ as was suggested by Thompson & Turner (1975) would lead to $D \propto (u_0^3/B_0)^{\frac{4}{11}}$.

In figure 9 the observed mixed-layer depths shown in figure 5 are replotted according to equation (4.6). The solid line is that given by (4.6) with $r = 2{\cdot}2$ the value obtained in § 2. The value of $u_0 z_0$ was evaluated from the grid parameters using (2.1). There are two points to note about this figure. First, the scatter is much reduced compared with that on figure 5 which indicates that this is an appropriate way to scale the data. Secondly, the actual numerical value of the mixed-layer depth is well predicted by (4.6) provided $D \lesssim 15$ cm. When $D \gtrsim 15$ cm the mixed-layer depth is over-estimated by (4.6), and the slope of $\frac{2}{11}$, corresponding to a decay law of $u \propto z^{-\frac{3}{4}}$ seems more appropriate. In fact, the measurements of the r.m.s. turbulent velocity reported by Thompson & Turner (1975) indicate a change in the decay law from z^{-1} to $z^{-\frac{3}{4}}$ at about this distance from the grid (see their figure 6*a*). This change in the decay law results from the presence of weak, large scale motions which have a length scale

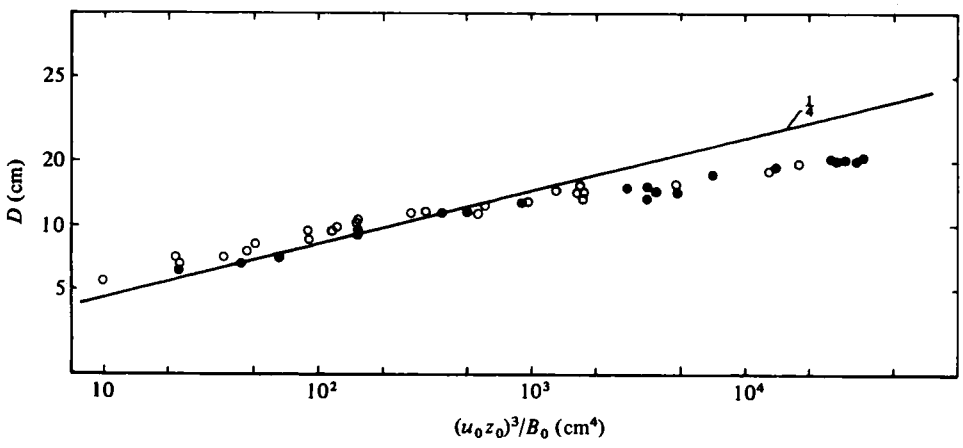

FIGURE 9. A log–log plot of the mixed-layer depth D against $(u_0 z_0)^3/B_0$. The solid straight line corresponds to equation (4.6) with $r = 2{\cdot}2$. ○, mass flux; ●, heat flux.

comparable to the half-width of the box (12·5 cm). This scale corresponds to the depth at which the decay law changes. Measurements made in a tank of larger cross-sectional dimensions showed no change in the decay law from $u \propto z^{-1}$ (Hopfinger & Toly 1976).

4.2. *Diffusion-flux Richardson number*

The flux Richardson number Rf is usually defined as the ratio of the rate of energy loss to the buoyancy forces to the rate of turbulent kinetic energy production by the Reynolds stresses acting on the mean shear. In the present problem there is no mean shear and the production of turbulent kinetic energy is located at the grid plane. Turbulence at positions remote from the grid results from the diffusive flux, as described by the terms on the left-hand side of (4.1). Thus we define a diffusion-flux Richardson number Rf_D as the ratio of the buoyancy flux to the diffusive flux of turbulent kinetic energy and, using (4.2), we write

$$Rf_D = \frac{g\overline{w'\rho'}}{\rho r\, du^3/dz}. \tag{4.7}$$

Substituting from (4.3) and (4.5) and setting $r = 2{\cdot}2$, we get

$$Rf_D = \frac{B_0 z^4 (1 - z/D)}{6{\cdot}6(u_0 z_0)^3 - B_0 z^4 \left(\frac{2}{5}\frac{z}{D} - \frac{1}{4}\right)}. \tag{4.8}$$

Figure 10 shows the diffusion-flux Richardson number given by (4.8) as a function of z/D. Near the oscillating grid where the turbulence is being generated, Rf_D is small indicating that energy flux balance is mainly between diffusion and viscous dissipation. The value of Rf_D increases as the thermocline at $z = D$ is approached and the buoyancy forces extract more of the turbulent kinetic energy. In the limit $z \to D$, (4.8) gives $Rf_D \to 1$ in which case all of the kinetic energy would be extracted by the buoyancy forces. This result casts doubt on the validity of the model near the thermocline when the turbulent velocities become very small. In particular, the assumption that the viscous dissipation is given by $\epsilon = Au^3/l$ may no longer be appropriate because

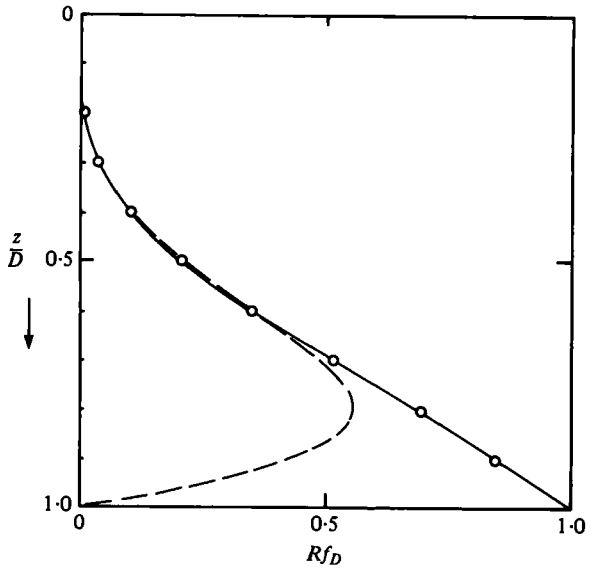

FIGURE 10. The variation in the diffusion-flux Richardson number with depth through the mixed layer calculated from equation (4.8). The broken line corresponds to Rf_D calculated using the turbulent energy flux in the absence of buoyancy.

u, and hence the Reynolds number, had dropped to a very small value in the vicinity of the thermocline. Also shown on figure 10 is the flux Richardson number calculated from (4.7) and using the turbulent energy flux which exists in the absence of buoyancy. The values of Rf_D are almost identical with those calculated from (4.8) provided $z/D \lesssim 0{\cdot}7$, but $Rf_D \to 0$ as $z/D \to 1$ because the buoyancy flux (but not the turbulent kinetic energy) is zero at $z = D$. This comparison of the two curves suggests that the buoyancy flux mainly affects the turbulence near the base of the mixed layer.

4.3. *Criterion of the onset of surface stratification*

We now apply the local energy flux balance to the case of 'bottom' stirring (see figure 1*c*). When the turbulence is generated at a distance D below the heating grid (4.2) gives

$$\frac{du^3}{dz'} = \frac{-b}{\beta}\frac{u^3}{z'} - \frac{1}{r}\frac{B_0}{D_1}(z' + D_1 - D), \tag{4.9}$$

where the lengths D, D_1, and z' are defined in figure 1(*c*). The solution of (4.9) with $u = u_0$ at $z' = z'_0$, for the case $z' \gg z'_0$ is

$$\left(\frac{u}{u_0}\right)^3 = \left(\frac{z'}{z_0}\right)^{-3}\left[1 - \frac{1}{r}\frac{B_0}{(u_0 z'_0)^3}\frac{z'^4}{D_1}\left(\frac{z'}{5} + \frac{D_1 - D}{4}\right)\right]. \tag{4.10}$$

According to (4.10) $u = 0$ at $z' = D$ when

$$B_0 = 5r(u_0 z'_0)^3/\gamma D^4, \tag{4.11}$$

where $\gamma = (5D_1 - D)/4D_1$, and $\gamma = 1$ when $D = D_1$. A non-dimensional parameter for correlating the data is thus

$$H = \gamma B_0 D^4/(u_0 z'_0)^3. \tag{4.12}$$

A measure of the dimensionless surface heating rate is given by

$$Q = \dot{T}_s(q_0/\rho C_p(D_1+d))^{-1}, \tag{4.13}$$

where $\dot{T}_s$ is the rate of increase in the surface temperature. The denominator is the rate of temperature increase which would be observed if the heat were mixed uniformly throughout the tank. Consequently, if there is no surface stratification $Q = 1$, whilst values of $Q > 1$ imply that a stable stratification has built up near the surface.

The non-dimensional surface heating rate Q is plotted logarithmically as a function of H on figure 11. The data cover a range of values of d, the distance of the heating grid from the surface and l, the integral scale of the turbulence. The depth D_1 was set at 25 cm and two values of the distance of the oscillating grid from the heating grid, $D = 12{\cdot}5$ cm and 18 cm, were used. In the three runs at the larger values of D, the depth slightly exceeds that over which the decay law $u \propto z^{-1}$ is valid. In any given experiment the value of Q remains equal to unity until a critical value of H is reached, after which surface stratification develops. The value of H at which the onset of surface stratification occurs depends on the ratio d/l when $d/l \lesssim 1{\cdot}5$, as the turbulence is then effected by the upper boundary. For $d/l \gtrsim 1{\cdot}5$, the critical value of H is close to 1·5, and beyond this value Q increases approximately linearly with H up to a value $H \sim 10$. Further increase in H leads to an asymptotic value of $Q = (D_1+d)/h$, where h is the thickness of the surface layer of temperature T_s. This final asymptotic state leads to a surface layer with a rapidly increasing temperature – a runaway stratification. The thickness of the surface layer depends on the distance d of the heating grid below the surface. Consequently, the asymptotic value of Q, and also the rate of increase of T_s with time once a stratified layer has been established, varies inversely with d.

The formation of a surface layer at the position of the heating grid is given by (4.11) to occur when $H = 5r$. Taking the value of $r = 2{\cdot}2$ as discussed in § 2 this implies that an interface forms when $H = 11$. This value corresponds closely with the point at which Q attains its asymptotic value – see figure 11.

The values of Q shown in figure 11 describe the initial rate of increase in surface temperature when a uniformly mixed layer is suddenly subjected to a stabilizing heat flux. As the temperature of the surface layer increases, the heat flux transmitted by conduction to the fluid below also increases and the rate of increase of T_s is reduced. An example of this behaviour is shown on figure 7. Under certain circumstances this heat flux from the surface layer becomes equal to the input heat flux and an equilibrium state with $Q = 1$, and a constant surface gradient, develops. The conditions under which this stratified equilibrium state ultimately develops are shown on figure 12. The open circles show the initial rate of increase in surface temperature as in figure 11, whilst the closed circles show the final value of Q. For $H \lesssim 7$ the system eventually adjusts to an equilibrium with $Q = 1$. At larger values of H the surface temperature always increases relative to the bulk temperature, and the strength of the stratification increases with time.

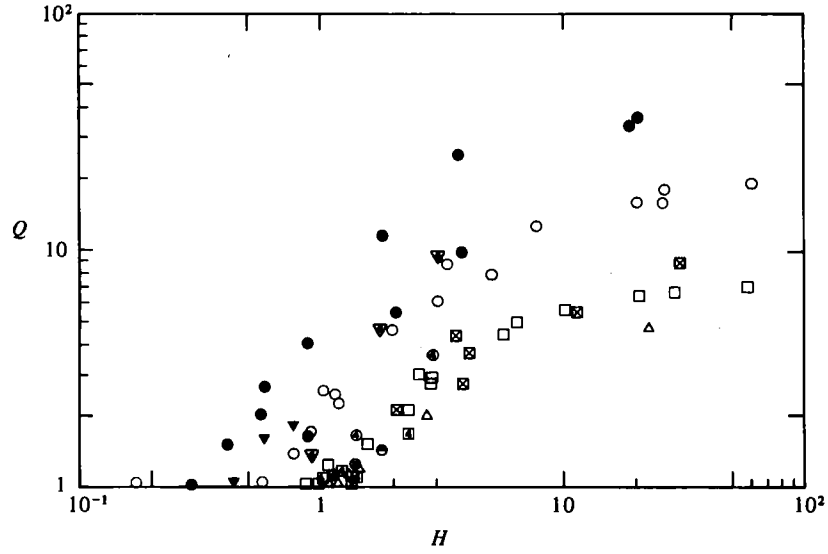

FIGURE 11. Rate of relative surface temperature increase Q, as a function of the parameter H in an initially homogeneous fluid column. ●, ▲, ○, □, △, ◓, S = 2·4 cm, D = 12·5 cm and d/l = 0·14, 0·24, 0·47, 1·41, 2·35, 3·3 respectively; ⊗, ⊠, S = 1 cm, D = 12·5 cm and d/l = 0·5 and 1·5; ▽, ⊙, ⊡, S = 4 cm, D = 18 cm, d/l = 0·25, 0·5, 1·5.

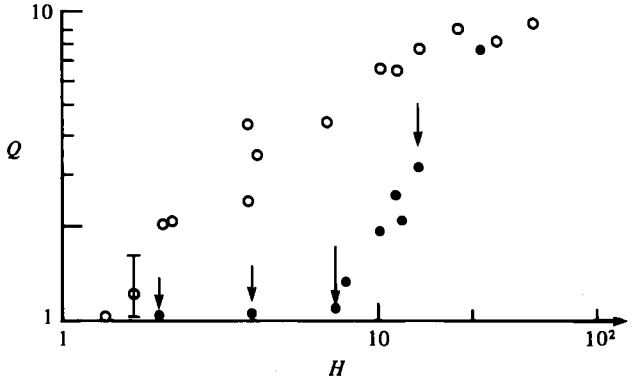

FIGURE 12. Rate of relative surface temperature increase Q as a function of H for S = 1 cm, D = 12·5 cm and d/l = 1·5. ○, initially homogeneous fluid column; ●, with existing surface gradient. The arrows indicate the direction of the change in time of Q from the initial value, when heating is applied to the homogeneous water column, to the final state after a surface gradient has developed.

5. Discussion and conclusions

The main results for the case of surface stirring are that, when the turbulent energy production and buoyancy flux are held constant, a mixed layer forms and its depth D remains constant in time. The mixed-layer depth is successfully predicted by a local energy-flux balance which explicitly takes into account the decay of turbulent energy with distance from the grid. This result emphasizes the fact that the effect of the buoyancy flux on the turbulence is strongest near the base of the mixed layer, and consequently it is necessary to relate the turbulence levels near the thermocline to the

surface parameters. As shown on figure 9 the mixed-layer depth scales on the local turbulence level, and changes in the neutral decay law in the tank are also reflected in the values of the mixed-layer depth.

A physical interpretation of the scaling law (4.6) is obtained by writing it in terms of the local r.m.s. turbulent velocity scale u. In the mixed layer $u_0 z_0 = uz$, and so at the base of the mixed layer (4.6) becomes

$$D = 20ru^3/B_0. \tag{5.1}$$

Since the buoyancy flux is zero at the base of the mixed layer, a reasonable estimate of the local buoyancy flux B, is the value one integral scale above the thermocline. Then from (4.3) we have

$$B = \frac{l}{D} B_0 = \beta B_0. \tag{5.2}$$

Substituting (5.2) into (5.1) we get

$$D = 20r\beta u^3/B = au^3/B. \tag{5.3}$$

This result is the local equivalent to Kitaigorodskii's (1960) global energy argument (1.1). With the parameter values $r = 2{\cdot}2$, $\beta = 0{\cdot}1$ we get $a = 4{\cdot}4$, which is about twice the value obtained by Kitaigorodskii using surface parameters u_* and B_0. Although, as was pointed out the actual scaling law in terms of surface parameters (4.6) depends on the nature of the turbulent decay, the result (5.3) is independent of the decay law. Thus (5.3) should be valid in other contexts such as boundary layers. Consequently, in situations where the turbulence intensity is approximately uniform, the global arguments and local balances are equivalent. Therefore, the global energy estimates may work satisfactorily in shallow mixed layers, or in cases of tidal stirring in shallow water.

Recent observations by Kondo, Konechika & Yasuda (1978) in the lower atmosphere indicate even higher values of the coefficient a in (5.3). They find that for $u_* = 4{\cdot}8$ cm s^{-1}, $B_0 = 0{\cdot}8$ cm^2 s^{-3} that the mixed-layer depth D is 9·5 m, which implies that $a \simeq 7$. In this case D is within the constant stress layer, and so the global and local energy arguments are similar.

When the turbulence is generated near the bottom, a stabilizing buoyancy flux generates surface stratification whenever $H \gtrsim 1{\cdot}5$. The precise value of H at which surface stratification begins depends on the distance from the surface that the heat is put into the water column. When $d/l < 1{\cdot}5$, then the decay of the turbulence as it approaches the free surface allows the onset of stratification at smaller values of H, as shown on figure 11.

The criterion for the onset of surface stratification $H \simeq 1{\cdot}5$, when expressed in terms of the local velocity u, is

$$B_0 D/u^3 \simeq 1{\cdot}5. \tag{5.4}$$

In tidal regions, changes from a well-mixed zone to a zone with surface stratification follow approximately contours of $D/|U|^3$ (Simpson & Hunter 1974) where $|U|$ is the r.m.s. velocity over a tidal cycle. If u can be taken a proportional to $|U|$, this behaviour agrees with relation (5.4). A comparison with Simpson & Hunter's results indicates that quantitative agreement would be obtained if $u/|U| \simeq 2 \times 10^{-2}$.

It should be emphasized, however, that the criterion for the onset of surface strati-

fication is applicable only when the initial water column is homogeneous. In general, the evolution of the stratification of water column depends upon its history and the presence of existing density gradients.

A stable density gradient is known to inhibit vertical turbulent mixing. In the light of the present experiments the question arises of whether the stable buoyancy flux resulting from entrainment across an interface, as studied by Turner (1968), is large enough to affect the turbulence in the mixed layer, away from the immediate vicinity of the interface. The buoyancy flux due to interfacial entrainment is given by $B_e = g\Delta\rho u_e/\rho$, where u_e is the entrainment velocity and $\Delta\rho$ the density jump across the interface. For temperature stratification the observed entrainment velocity is given by $u_e/u = cRi^{-1}$ where $Ri = g\Delta\rho l/\rho u^2$ is an interfacial Richardson number, and $c = 1{\cdot}0$ is a constant (Turner 1973, p. 291). Substituting the value B_e for the buoyancy flux B_0 in (4.12) and using $u_0 z_0' = ul/\beta$, we find $H = \frac{1}{4}\beta^{-1}(u_e/u)\,Ri$. Turner's experimental results then give $H \doteq c/\beta$ which takes values $H \lesssim 10$ for $\beta \gtrsim 0{\cdot}1$. From the data shown on figure 12 it can be seen that the turbulence is significantly affected by the buoyancy flux for values $H \gtrsim 10$. Consequently, it is concluded that although the stabilizing buoyancy flux may have some effect on the turbulence in the mixed layer, these modifications are small compared with the effect of the interface itself.

REFERENCES

HOPFINGER, E. J. & TOLY, J.-A. 1976 Spatially decaying turbulence and its relation to mixing across density interfaces. *J. Fluid Mech.* **78**, 155–175.

KANTHA, L. H. & LONG, R. R. 1980 Turbulent mixing with stabilizing surface buoyancy flux. *Phys. Fluids* **23**, 2142–2143.

KITAIGORODSKII, S. A. 1960 On the computation of the thickness of the wind-mixing layer in the ocean. *Bull. Acad. Sci. U.S.S.R. Geophys. Ser.* **3**, 284–287.

KONDO, J., KONECHIKA, O. & YASUDA, N. 1978 Heat and momentum transfers under strong stability in the atmospheric surface layer. *J. Atmos. Sci.* **35**, 1012–1021.

KRAUS, E. B. 1977 *Modelling and Prediction of the Upper Layers of the Ocean.* Pergamon.

KRAUS, E. B. & TURNER, J. S. 1967 A one-dimensional model of the seasonal thermocline. II. The general theory and its consequences. *Tellus* **19**, 98–106.

LINDEN, P. F. 1975 The deepening of the mixed layer in a stratified fluid. *J. Fluid Mech.* **71** 385–405.

LONG, R. R. 1978 Theory of turbulence in a homogeneous fluid induced by an oscillating grid. *Phys. Fluids* **21**, 1887–1888.

MCDOUGALL, T. J. 1979 Measurements of turbulence in a zero-mean-shear mixed layer. *J. Fluid Mech.* **94**, 409–431.

SIMPSON, J. H. & HUNTER, J. R. 1974 Fronts in the Irish Sea. *Nature* **250**, 404–406.

THOMPSON, S. M. & TURNER, J. S. 1975 Mixing across an interface due to turbulence generated by an oscillating grid. *J. Fluid Mech.* **67**, 349–368.

TURNER, J. S. 1968 The influence of molecular diffusivity on turbulent entrainment across a density interface. *J. Fluid Mech.* **33**, 639–656.

TURNER, J. S. 1973 *Buoyancy effects in fluids.* Cambridge University Press.

TURNER, J. S. & KRAUS, E. B. 1967 A one-dimensional model of the seasonal thermocline. I. A laboratory experiment and its interpretation. *Tellus* **19**, 88–97.